Computer Assisted Mechanics and Engineering Sciences, **18**: 91–113, 2011.

Mathematical and numerical multi-scale modelling of multiphysics problems

Bernhard A. Schrefler, Daniela P. Boso, Francesco Pesavento
Department of Structural and Transportation Engineering, University of Padova
via F. Marzolo 9, 35131 Padova, Italy
e-mail: bas@dic.unipd.it, boso@dic.unipd.it, pesa@dic.unipd.it

Dariusz Gawin, Marek Lefik
Technical University of Łódź
Al. Politechniki 6, 93-590 Łódź, Poland
e-mail: dariusz.gawin@p.lodz.pl, marek.lefik@p.lodz.pl

In this paper we discuss two multi-scale procedures, both of mathematical nature as opposed to purely numerical ones. Examples are shown for the two cases. Attention is also devoted to thermodynamical aspects such as thermodynamic consistency and non-equilibrium thermodynamics. Advances for the first aspect are obtained by adopting the thermodynamically constrained averaging theory TCAT as shown in the case of a stress tensor for multi-component media. The second aspect has allowed to solve numerically, with relative ease, the case of non-isothermal leaching. The absence of proofs of thermodynamic consistency in case of asymptotic theory of homogenization with finite size of the unit cell is also pointed out.

Keywords: multiphysics problems, multi-scale models, asymptotic homogenisation.

1. Introduction

Multi-scale methods are nowadays very popular in the community dealing with computational methods in applied sciences and engineering. At the extreme, these methods allow to bridge the scales from quantum mechanics to the continuum at macroscopic level [61]. In such instances the scale bridging method is mainly of numerical nature [77]. In multi-physics problems, however, it is often advantageous to use multi-scale procedures already at mathematical level when formulating the model. In this case, seldom more than two or three scales are involved. This is particularly the case of multi-physics problems with overlapping domains where diffusion, advection, adsorption, phase change, deformation, chemical reactions and other phenomena take place. In such a case a mathematical multi-scale approach is useful to obtain the proper form of the interaction and exchange terms among the fields. The purely macroscopic approaches often yield to confusion and to wrong forms of the interaction terms. Using appropriate approaches such as the hybrid mixture theory [38] which in fact is an averaging method, or the thermodynamically constrained averaging theory TCAT [39] allows assuring that the second law of thermodynamics is satisfied. In the hybrid mixture theory the system thermodynamics is postulated directly at the average scale (i.e., the macroscale) and thus does not account for some of the sub-scale deviations in thermodynamic properties; and the thermodynamic statements do not necessarily downscale to the microscale. On the other hand, the thermodynamically constrained averaging theory TCAT involves averaging established micro-scale thermodynamic principles to the macroscale. In doing so, it inherently assures consistency between micro-scale and macro-scale forms.

Thermodynamic consistency of the mathematical model improves the performance of the ensuing numerical model. This is due to the fact that unwanted and uncontrolled dissipation is eliminated. The fact that thermodynamically consistent models behave better than others is known from Computational Fluid Dynamics (CFD) where numerical dissipation is introduced for this purpose. Numerical dissipation enters stability estimates which, physically speaking, can be understood as energy estimates. But, if well designed, the same dissipation enters in entropy estimates and helps to guarantee that entropy is never decreasing. For a compressible flow setting, see Hughes et al. [48, 49]. A more mathematically oriented exposition of the concept is due to Johnson and Szepessy [51] and Szepessy [73], where the relationship between dissipation and entropy inequalities is shown for hyperbolic equations. More recently, the connection between entropy conditions and numerical dissipation is being exploited by Guermond [42].

In the computational fluid-solid interaction community (FSI, interaction in the domain) the thermodynamical consistency is investigated by Coussy [19, 20], Baggio et al. [1], Schrefler [71], Hutter et al.[50], de Boer et al. [21], Borja [4].

We shall show how such consistency can be obtained in FSI. With an appropriate multi-scale procedure such as TCAT, a remarkable result can be achieved which cannot be obtained with a macro-scale continuum theory of thermodynamics [4]. As a second case, we discuss the adoption of non-equilibrium thermodynamics which allows to obtain correct models, for instance in non isothermal leaching. Such an extension from the isothermal case has not been obtained with thermodynamic equilibrium assumptions.

Finally, another case of interest is the asymptotic theory of homogenisation which is often used in solid mechanics problems, [5, 6, 18, 70, 80]. The expansion is usually truncated after a few terms. What matters here in conserving the thermodynamical consistency is the size of the unit cell. As long as it is infinitesimally small it is generally accepted that the 0(1) theory is as good as anything else. The problem is finite size of the cell which usually appears in numerical exploitation of the method. Here the question is still open.

We shall show some examples for mathematical and numerical multi-scale methods belonging to stress measures in partially saturated media and their effects on drying shrinkage modelling in concrete, to calcium leaching in concrete, and to three-scale homogenisation with application to nuclear fusion technology.

2. Space averaging for multiphase porous materials

The multiphase porous medium model used as example is assumed far from thermodynamic equilibrium state. It is treated within the framework of averaging theories by Hassanizadeh and Gray [38, 44, 45, 47], starting from microscopic level and applying the mass-, area- and volume-averaging operators to the local form of balance equations.

The porous material is considered to be a multiphase medium where the voids of the solid skeleton could be filled with various combinations of liquid- and gas-phases (Fig. 1). In typical

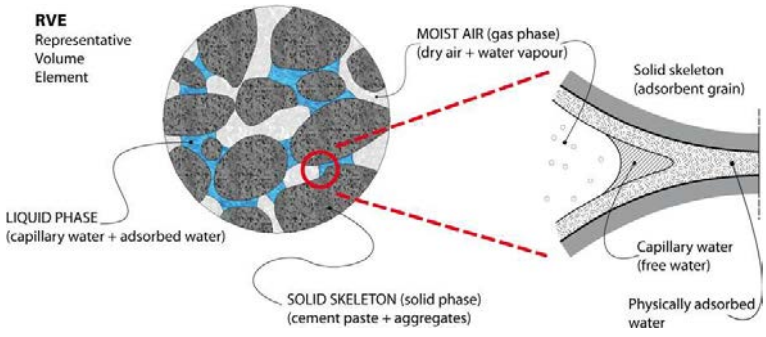

Fig. 1. Schematic representation of the moist concrete as a multiphase porous material.

situations, like for example concrete or soils, the fluids filling pore space are the moist air (mixture of dry air and vapor), capillary water and physically adsorbed water. The chemically-bound water, if present (like, e.g., in concrete), is considered to be part of the solid skeleton until it is released on heating to high temperature.

2.1. Microscopic balance equations

In this section, the averaging procedure of conservation equations is summarised [38, 44, 45, 47] which traditionally positions thermodynamic statements directly at the macroscale. This procedure is not sufficient for obtaining a correct form of the stress tensor as shown in Subsec. 2.3. The fluid phases and the solid are separated at microscopic level by interfaces and the latter ones by contact lines. As underlined in [38], the interfaces between the constituents and their thermodynamic properties are important to consider properly constitutive relationships; thus, they are taken into account in defining the general form of the model. The contact lines are supposed to not posses any thermodynamic property, even if they allow for exchange of properties between interfaces. The solid phase is assumed to be in contact with all fluids in the pores. In the following, the bulk phases are indicated with Greek letters ($\alpha, \beta = w, g, s$, where w means the water, g the gas, and s the solid skeleton), while for the interfaces and contact lines some combinations of two and three Greek letters have been used, respectively.

For a thermodynamic property, ψ, the balance equation within the bulk α-phase may be written as follows [38, 44]:

$$\frac{\partial\left(\rho^{\alpha}\psi\right)}{\partial t}+\operatorname{div}\left(\rho^{\alpha}\psi\,\mathbf{v}^{\alpha}\right)=\operatorname{div}\mathbf{i}_{\psi}+\rho^{\alpha}\mathbf{b}_{\psi}+\rho^{\alpha}\mathbf{G}_{\psi} \tag{1}_1$$

and for the $\alpha\beta$-interface it has a similar form:

$$\frac{\partial\left(\Gamma^{\alpha\beta}\psi\right)}{\partial t}+\operatorname{div}\left(\Gamma^{\alpha\beta}\psi\mathbf{w}^{\alpha\beta}\right)=\operatorname{div}\mathbf{i}_{\psi}+\Gamma^{\alpha\beta}\mathbf{b}_{\psi}+\Gamma^{\alpha\beta}\mathbf{G}_{\psi}, \tag{1}_2$$

where ρ^{α} is the density of the α phase, $\Gamma^{\alpha\beta}$ the surface excess mass density of $\alpha\beta$-interface, $\mathbf{v}^{\alpha}$ the local value of the velocity field of the α phase in a fixed point in space, $\mathbf{w}^{\alpha\beta}$ the local value of the velocity field of the interface $\alpha\beta$, $\mathbf{i}_{\psi}$ is the flux vector associated with ψ, $\mathbf{b}_{\psi}$ the external supply of ψ and $\mathbf{G}_{\psi}$ is the net production of ψ. Fluxes are positive as outflows.

The thermodynamic quantity ψ, to be introduced into Eq. (1), can be mass, momentum, angular momentum, energy or entropy. The relevant thermodynamic properties ψ for the different balance equations and values assumed by $\mathbf{i}_{\psi}$, $\mathbf{b}_{\psi}$, and $\mathbf{G}_{\psi}$ are listed in Table 1, where E is the specific intrinsic energy, λ the specific entropy, $\mathbf{t}_m^{\alpha}$ and $\mathbf{s}_m^{\alpha\beta}$ the microscopic stress tensors for the bulk and interfaces, respectively, $\mathbf{q}$ the heat flux vector, $\mathbf{\Phi}$ the entropy flux, $\mathbf{g}$ the external momentum supply related to gravitational forces, h the intrinsic heat source, S the intrinsic entropy source and

Table 1. Thermodynamic properties for the microscopic mass balance equations.

Quantity		ψ	$\mathbf{i}_{\psi}$	$\mathbf{b}_{\psi}$	$\mathbf{G}_{\psi}$
Mass	bulk phase or interface	1	0	0	0
Momentum	bulk phase	$\mathbf{v}^{\alpha}$	$\mathbf{t}_m^{\alpha}$	$\mathbf{g}$	0
	interface	$\mathbf{w}^{\alpha\beta}$	$\mathbf{s}_m^{\alpha\beta}$	$\mathbf{g}^{\alpha\beta}$	0
Energy	bulk phase	$E^{\alpha}+0.5\mathbf{v}^{\alpha}\cdot\mathbf{v}^{\alpha}$	$\mathbf{t}_m^{\alpha}\mathbf{v}^{\alpha}-\mathbf{q}^{\alpha}$	$\mathbf{g}\cdot\mathbf{v}^{\alpha}+h^{\alpha}$	0
	interface	$E^{\alpha\beta}+0.5\mathbf{w}^{\alpha\beta}\cdot\mathbf{w}^{\alpha\beta}$	$\mathbf{s}_m^{\alpha\beta}\mathbf{w}^{\alpha\beta}-\mathbf{q}^{\alpha\beta}$	$\mathbf{g}^{\alpha\beta}\cdot\mathbf{w}^{\alpha\beta}+h^{\alpha\beta}$	0
Entropy	bulk phase	λ^{α}	$\mathbf{\Phi}^{\alpha}$	S^{α}	φ^{α}
	interface	$\lambda^{\alpha\beta}$	$\mathbf{\Phi}^{\alpha\beta}$	$S^{\alpha\beta}$	$\varphi^{\alpha\beta}$

φ denotes an increase of entropy. The quantities related to the solid phases have upper index α, and those for the interfaces $\alpha\beta$. The constituents are assumed to be microscopically non-polar; hence, the angular momentum balance equation has been omitted here. This equation shows, however, that the stress tensors are symmetric.

2.2. Macroscopic balance equations

The macroscopic balance equations are obtained by applying appropriate space averaging operators (for the so-called Representative Volume Element – RVE, Fig. 1) to the equations at micro-level, Eq. (1), while the constitutive laws are defined directly at the upper scale, according to the so-called Hybrid Mixture Theory (HMT) originally proposed by Hassanizadeh and Gray [45–47].

The chosen procedure does not exclude the use of a numerical multi-scale approach (i.e., numerical averaging in RVE) in the formulation of the material properties, which nowadays is often used for solving problems involving multi-physics aspects in material mechanics.

After application of HMT theory (i.e., space averaging in RVE), the set of governing equations at macroscopic level is as follows (for a detailed description of the procedure see [38, 44, 71]).

– *Mass balance equation for bulk phases and interfaces:*

$$\frac{D^{\alpha}\eta^{\alpha}\rho^{\alpha}}{Dt} + \eta^{\alpha}\rho^{\alpha}\mathrm{div}\,\mathbf{v}^{\alpha} = \sum_{\beta}\widehat{e}^{\alpha}_{\alpha\beta}, \tag{2}$$

$$\frac{D^{\alpha\beta}a^{\alpha\beta}\Gamma^{\alpha\beta}}{Dt} + a^{\alpha\beta}\Gamma^{\alpha\beta}\mathrm{div}\,\mathbf{w}^{\alpha\beta} = -\widehat{e}^{\alpha}_{\alpha\beta} - \widehat{e}^{\beta}_{\alpha\beta} + \widehat{e}^{\alpha\beta}_{\alpha\beta\gamma}, \tag{3}$$

where η^{α} means the volumetric fraction of the α phase, $\widehat{e}^{\alpha}_{\alpha\beta}$ the rate of mass transfer to the bulk phase α from interface $\alpha\beta$, $a^{\alpha\beta}$ the area of $\alpha\beta$ interface per averaging volume, $\Gamma^{\alpha\beta}$ the macroscopic excess of surface mass density for $\alpha\beta$-interface, $\widehat{e}^{\alpha\beta}_{\alpha\beta\gamma}$ the rate of mass transfer to the interface $\alpha\beta$ from the contact line $\alpha\beta\gamma$.

The mass source terms on the right hand side (RHS) of Eq. (2) correspond to an exchange of mass with interfaces separating individual phases (phase changes) and couple these equations with the corresponding balance equations written for the interfaces. The last term in Eq. (3) describes mass exchange of the interfaces with their contact line. Since we have three phases composing the medium, there is only one contact line (which does not have any thermodynamic property). In Eq. (3), $\Gamma^{\alpha\beta}$ is used for taking into account the transition in density from one phase to another.

– *Momentum balance equations for the bulk phases and interfaces:*

$$\eta^{\alpha}\rho^{\alpha}\frac{D^{\alpha}\mathbf{v}^{\alpha}}{Dt} - \mathrm{div}\,(\eta^{\alpha}\mathbf{t}^{\alpha}) - \eta^{\alpha}\rho^{\alpha}\mathbf{g} = \sum_{\beta}\widehat{\mathbf{T}}^{\alpha}_{\alpha\beta}, \tag{4}$$

$$\begin{aligned} a^{\alpha\beta}\Gamma^{\alpha\beta}\frac{D^{\alpha\beta}\mathbf{w}^{\alpha\beta}}{Dt} - \mathrm{div}\left(a^{\alpha\beta}\mathbf{s}^{\alpha\beta}\right) - a^{\alpha\beta}\Gamma^{\alpha\beta}\mathbf{g}^{\alpha\beta} \\ = -\left(\widehat{\mathbf{T}}^{\alpha}_{\alpha\beta} + \widehat{e}^{\alpha}_{\alpha\beta}\mathbf{w}^{\alpha,s}\right) - \left(\widehat{\mathbf{T}}^{\beta}_{\alpha\beta} + \widehat{e}^{\beta}_{\alpha\beta}\mathbf{w}^{\beta,s}\right) + \left(\widehat{e}^{\alpha}_{\alpha\beta} + \widehat{e}^{\beta}_{\alpha\beta}\right)\mathbf{w}^{\alpha\beta,s} + \widehat{\mathbf{S}}^{\alpha\beta}_{\alpha\beta\gamma}, \end{aligned} \tag{5}$$

where $\mathbf{t}^{\alpha}$ means the partial stress tensor of the α-phase, $\mathbf{g}$ the gravity acceleration, $\widehat{\mathbf{T}}^{\alpha}_{\alpha\beta}$ the body momentum supply to the bulk phase α from the $\alpha\beta$-interfaces, $\mathbf{s}^{\alpha\beta}$ the surface stress tensor, $\mathbf{g}^{\alpha\beta}$ the acceleration of the $\alpha\beta$ interface, $\mathbf{v}^{\alpha,s}$ the relative velocity of the α-phase with respect to the

solid phase "s", $\mathbf{w}^{\alpha,\alpha\beta}$ the relative velocity of the α-phase with respect to $\alpha\beta$-interface, $\widehat{\mathbf{S}}^{\alpha\beta}_{\alpha\beta\gamma}$ the momentum supply to the $\alpha\beta$-interfaces from the $\alpha\beta\gamma$-contact line.

The RHS terms in Eq. (4) describe the supply of momentum from the interfaces, i.e., related to phase changes. In this equation, the surface stress tensor, $\mathbf{s}^{\alpha\beta}$, is symmetric.

– Energy balance equations for the bulk phases and the interfaces:

$$\eta^\alpha \rho^\alpha \frac{D^\alpha E^\alpha}{Dt} - \eta^\alpha \mathbf{t}^\alpha \colon \operatorname{grad} \mathbf{v}^\alpha - \operatorname{div}\left(\eta^\alpha \mathbf{q}^\alpha\right) - \eta^\alpha \rho^\alpha h^\alpha = \sum_\beta \widehat{Q}^\alpha_{\alpha\beta}, \tag{6}$$

$$\begin{aligned} a^{\alpha\beta} \Gamma^{\alpha\beta} \frac{D^{\alpha\beta} E^{\alpha\beta}}{Dt} - a^{\alpha\beta} \mathbf{s}^{\alpha\beta} \colon \operatorname{grad} \mathbf{v}^{\alpha\beta} - \operatorname{div}\left(a^{\alpha\beta} \mathbf{q}^{\alpha\beta}\right) - a^{\alpha\beta} \Gamma^{\alpha\beta} h^{\alpha\beta} \\ = -\left[\widehat{Q}^\alpha_{\alpha\beta} + \widehat{\mathbf{T}}^\alpha_{\alpha\beta} \cdot \mathbf{v}^{\alpha,\alpha\beta} + \widehat{e}^\alpha_{\alpha\beta}\left(\left(E^\alpha - E^{\alpha\beta}\right) + \frac{1}{2}\left(\mathbf{v}^{\alpha,\alpha\beta}\right)^2\right)\right] \\ - \left[\widehat{Q}^\beta_{\alpha\beta} + \widehat{\mathbf{T}}^\beta_{\alpha\beta} \cdot \mathbf{v}^{\beta,\alpha\beta} + \widehat{e}^\beta_{\alpha\beta}\left(\left(E^\beta - E^{\alpha\beta}\right) + \frac{1}{2}\left(\mathbf{v}^{\beta,\alpha\beta}\right)^2\right)\right] + \widehat{Q}^{\alpha\beta}_{\alpha\beta\gamma}, \end{aligned} \tag{7}$$

where E^α is the internal energy of bulk phase α, $\mathbf{q}^\alpha$ the heat flux vector for the bulk phase α, h^α the heat source in the bulk phase α, $\widehat{Q}^\alpha_{\alpha\beta}$ the body supply of the heat to the bulk phase α from the interface $\alpha\beta$, $\widehat{Q}^{\alpha\beta}_{\alpha\beta\gamma}$ the body supply of the heat to the interface $\alpha\beta$ from the contact line $\alpha\beta\gamma$.

The source terms in Eq. (6) describe supply of heat to bulk phase from the interfaces, related to phase changes. The terms in square brackets in Eq. (7) describe the energy supply from the bulk phase to the interface, energy associated with momentum supply and energy related to mass supply because of phase changes.

– Entropy balance equations for the bulk phases and for the interfaces:

The entropy fluxes are defined here as heat fluxes divided by temperature T (otherwise a constitutive relationship is needed) and the entropy external supply due solely to external energy sources is considered, i.e., assuming the hypothesis of simple thermodynamic processes. Thus, the entropy balance for the bulk phases and interfaces may be expressed as follows [38, 44, 71]:

$$\eta^\alpha \rho^\alpha \frac{D^\alpha \lambda^\alpha}{Dt} - \operatorname{div}\left(\eta^\alpha \frac{\mathbf{q}^\alpha}{T^\alpha}\right) - \eta^\alpha \rho^\alpha \frac{h^\alpha}{T^\alpha} = \sum_\beta \widehat{\mathbf{\Phi}}^\alpha_{\alpha\beta} + \Lambda^\alpha, \tag{8}$$

$$\begin{aligned} a^{\alpha\beta} \Gamma^{\alpha\beta} \frac{D^{\alpha\beta} \lambda^{\alpha\beta}}{Dt} - \operatorname{div}\left(a^{\alpha\beta} \frac{\mathbf{q}^{\alpha\beta}}{T^{\alpha\beta}}\right) - a^{\alpha\beta} \Gamma^{\alpha\beta} \frac{h^{\alpha\beta}}{T^{\alpha\beta}} \\ = -\left[\widehat{\mathbf{\Phi}}^\alpha_{\alpha\beta} + \widehat{e}^\alpha_{\alpha\beta}\left(\lambda^\alpha - \lambda^{\alpha\beta}\right)\right] - \left[\widehat{\mathbf{\Phi}}^\beta_{\alpha\beta} + \widehat{e}^\beta_{\alpha\beta}\left(\lambda^\beta - \lambda^{\alpha\beta}\right)\right] + \widehat{\mathbf{\Phi}}^{\alpha\beta}_{\alpha\beta\gamma} + \Lambda^{\alpha\beta}, \end{aligned} \tag{9}$$

where λ^α is the specific entropy of the α-phase, T^α the absolute temperature of the α-phase, $\widehat{\mathbf{\Phi}}^\alpha_{\alpha\beta}$ the body entropy supply to the bulk phase α from the interface $\alpha\beta$, Λ^α the rate of net production of entropy of the α-phase, $T^{\alpha\beta}$ the absolute temperature of the $\alpha\beta$-interface, $\widehat{\mathbf{\Phi}}^{\alpha\beta}_{\alpha\beta\gamma}$ the body entropy supply to the interface $\alpha\beta$ from the contact line $\alpha\beta\gamma$, $\Lambda^{\alpha\beta}$ the rate of net production of entropy of the $\alpha\beta$-interface.

The two first terms in RHS of Eq. (8) describe the entropy supply to the bulk phases from the interfaces, while the last one is the rate of net production of entropy in the bulk phase. The terms in parentheses in the RHS of Eq. (9) describe the supply of entropy from the interfaces and the one resulting from the mass supply (phase change), the last but one accounts for entropy supply

to the interface from the contact line and the last one is the rate of net production of entropy in the interface.

The terms related to exchange of mass, momentum, energy and entropy between interfaces via the contact lines must satisfy some restrictions, because the contact lines do not possess any thermodynamic properties as already stated. Thus, the following relations hold:

$$\begin{aligned}
&\sum_{\alpha\beta} \widehat{e}^{\alpha\beta}_{wgs} = 0,\\
&\sum_{\alpha\beta} \left(\widehat{\mathbf{s}}^{\alpha\beta}_{wgs} + \widehat{e}^{\alpha\beta}_{wgs} \mathbf{w}^{\alpha\beta} \right) = 0,\\
&\sum_{\alpha\beta} \left[\widehat{Q}^{\alpha\beta}_{wgs} + \widehat{\mathbf{s}}^{\alpha\beta}_{wgs} \cdot \mathbf{w}^{\alpha\beta} + \widehat{e}^{\alpha\beta}_{wgs} \left(E^{\alpha\beta} + \frac{1}{2} \left(\mathbf{w}^{\alpha\beta} \right)^2 \right) \right] = 0,\\
&\sum_{\alpha\beta} \left(\widehat{\mathbf{\Phi}}^{\alpha\beta}_{wgs} + \widehat{e}^{\alpha\beta}_{wgs} \lambda^{\alpha\beta} \right) = 0.
\end{aligned} \tag{10}$$

The full development and the final form of the model equations, specific for different multiphase porous media is presented elsewhere: for partially saturated soils in [24, 25, 37, 69], for building materials in [24, 25], for maturing concrete in [30, 31, 33], for concrete at high temperature in [26–29, 32, 65], and for concrete exposed to chemical degradation in [34–36, 53, 54, 65].

2.3. Effective stress principle

When analysing the stress state and the deformation of the multi-phase porous media it is necessary to consider not only the action of an external load, but also the pressure exerted on the skeleton by fluids present in its voids. Hence, the total (nominal) stress tensor $\mathbf{t}^{tot}$ acting in a point of the porous medium may be split into the effective stress $\eta^s \mathbf{t}^s$, which accounts for stress effects due to changes in porosity, spatial variation of porosity and the deformations of the solid matrix, and a part accounting for the solid phase pressure exerted by the pore fluids, [38, 40, 41, 65]:

$$\mathbf{t}^{tot} = \eta^s \mathbf{t}^s - \alpha P^s \mathbf{I}, \tag{11}$$

where $\mathbf{I}$ is the second order unit tensor, α the Biot coefficient and P^s is some measure of solid pressure acting in the system, also simply called a solid pressure. The above definition of total stress tensor has been obtained in [40, 65] from the exploitation of second Thermodynamics principle in the form given in [41], considering equations (2)–(10).

Many different forms of P^s have been proposed in the past decades in Geomechanics, but considering that concrete has a fine microstructure, i.e., the interactions between molecules of water and concrete skeleton on micro-structural level are rather complex, the formulation by Gray and Schrefler [41], which takes into account the degree of contact of each fluid phase with the solid one, has been adopted here. Only using TCAT formalism has allowed to show the conditions under which this split (11) is thermodynamically consistent. Prior to the development of the TCAT approach for geomechanical applications, it had been stated [4] that no continuum theory of thermodynamics had shown the validity of this stress form. The stress equations provided by TCAT guarantee thermodynamic consistency that cannot be achieved by positioning the macro-scale thermodynamics directly at the macroscale by averaging of conservation equations with rational thermodynamics. TCAT provides not only the definition of the stress tensor and effective stress, but also the definition of the Biot coefficient and P^s, p^s. Including the interface in the analysis allows to interpret the Biot coefficient as the ratio of the hydrostatic part of the total stress tensor ($\mathbf{t}^{tot}$) to the normal force exerted on the solid surface by the surrounding fluids, i.e., $-\langle \mathbf{n}_s \mathbf{t}^s_m \mathbf{n}_s \rangle^{ss}$

$$\alpha = -\frac{p^{total}}{\langle \mathbf{n}_s \mathbf{t}^s_m \mathbf{n}_s \rangle^{ss}} = 1 - \frac{\widetilde{K}_T}{\widetilde{K}_S}. \tag{12}$$

This relationship accounts for different values of bulk modulus for solid phase (grain) and the skeleton, $\widetilde{K}_S$ and $\widetilde{K}_T$, respectively. Here, $\mathbf{t}^s_m$ is the stress tensor of the solid phase at microscopic level, $\mathbf{n}_s$ is the unit vector normal to the solid phase in each point, while the Macaulay brackets $\langle\ \rangle^{ss}$ indicate an averaging over the solid surface. With these results, P^s is selected to be the average normal force exerted on the solid surface by the fluids in the pore space:

$$P^s = -\left\langle \mathbf{n}_s \mathbf{t}^s_m \mathbf{n}_s \right\rangle^{ss}. \tag{13}$$

By considering the interfaces and by formulating the model from the micro-level, the following form of the so-called "standard solid pressure", $p^{s,}$, is obtained [41]:

$$p^s = x^{ws}_s p^w + x^{gs}_s p^g + x^{ws}_s \gamma^{ws} J^s_{ws} + x^{gs}_s \gamma^{gs} J^s_{gs}, \tag{14}$$

where x^{ws}_s and x^{gs}_s are the fractions of skeleton area in contact with water and gas, respectively, while J^s_{ws} and J^s_{gs} are the curvature of the water/solid and gas/solid interfaces in that order. γ^{ws} and γ^{gs} are surface tension-like terms. The two forms of the solid pressure are related one to each other by means of:

$$p^s = \alpha P^s. \tag{15}$$

For further details see [38, 40, 41, 65].

By using the following simplified version of the capillary pressure, valid at thermodynamic equilibrium and neglecting the direct contribution of the fluid-solid interfaces, we obtain:

$$p^c \equiv p^g - p^w = \Pi^f - \gamma^{wg} J^w_{wg}. \tag{16}$$

Equation (14) can be transformed into:

$$p^s = p^g + x^{ws}_s \gamma^{wg} J^w_{wg} - x^{ws}_s \Pi^f + x^{ws}_s \gamma^{ws} J^s_{ws} + (1 - x^{ws}_s)\ \gamma^{gs} J^s_{gs}. \tag{17}$$

Equation (16) considers the disjoining pressure Π^f and can be applied in the hygroscopic region (i.e., when the saturation level is lower than the solid saturation point and the water is present only as a thin film on the skeleton surface) as well as in the non-hygroscopic region (i.e., for higher levels of moisture content, for which saturation values exceed the solid saturation point).

In Eq. (17), one can recognize terms corresponding to the main physical phenomena leading to concrete shrinkage: the first term on the r.h.s describes an effect of gas pressure, the second one of capillary tension, the third one of disjoining pressure, and the last two terms, resulting from the action of surface tension of solids on the interfaces with the pore fluids, are negligible. Taking into account such simplifications and relation (16), the so-called "effective stress principle", i.e., Eq. (11), can be rewritten in the following simplified manner [33, 41]:

$$\eta^s \mathbf{t}^s = \mathbf{t}^{total} + (p^g - x^{ws}_s p^c)\, \mathbf{I}. \tag{18}$$

3. Multi-scale modelling

In the case when more specific information on the microstructure is given or available (not only volume fractions as in most of porous materials like soils, ceramics etc...), more sophisticated tools are needed to take it into account [52]. Materials with internal structure have in common that each structural level plays its own role in the global response: the material behaviour is controlled by the physical phenomena which take place at the various scales and by the interaction of these phenomena across scales. Single-scale models, usually at macroscale, make use of constitutive equations which should reflect the behaviour of the underlying scales. These constitutive equations are generally of a phenomenological type. An alternative to the use of constitutive equations at a single (macro) scale is provided by multi-scale modelling, in which the relevant physics is explicitly

captured on multiple spatial and temporal scales [66]. The outputs of multi-scale material modelling are usually effective properties which are used at higher scales. This analysis may also span over several scales where the output from the preceding lower level is used as input for the subsequent level.

In the case of material multi-scale modelling it is usually of interest to proceed from the lower scales upward to obtain the homogenized material properties; however, it is also very important to be able to step down through the scales until the desired scale of the real, not homogenised material is reached. This technique is commonly known as "unsmearing" or "localisation". Usually in a global analysis both aspects have to be pursued.

The most common methods for scale bridging are self-consistent methods and asymptotic analysis. Self-consistent methods give estimates for effective material properties as a function of some parameter such as for instance the volume ratio of the inclusions in a matrix. These methods go back to the works by Voigt [75], Reuss [67] and Eshelby [22] and have been extended by Hashin and Strikmann [43], and Mori and Tanaka [62]. These methods fail when the volume ratio is not able to characterise sufficiently well the geometry of the microstructure. Further work can be found in Kröner [55, 56] and Willis [76]. A new development for the non linear behaviour in the coupled thermo-mechanical field has been recently published in [9, 12] and [57]. An alternative approach for scale bridging is asymptotic analysis of media with periodic (or quasi-periodic) structure at micro-level, also called asymptotic theory of homogenisation.

3.1. Asymptotic theory of homogenization

The asymptotic analysis does not only permit to obtain equivalent material properties, but allows also to solve the full structural problem down to stresses in the constituent materials at micro (or local) scale. It is mostly applied to linear two-scale problems, but it can be extended to non-linear analysis and to several scales as will be shown in Subsec. 3.6. We do not intend to give here a full account of the underlying theory. The interested reader will find in [3] and [70] the rigorous formulation of the method, its application in many fields and further references.

In this study, composites with a regular or nearly regular structure are considered. Having sufficiently regular heterogeneities enables us to assume a periodic structure for the composite. It should be emphasized that in comparison with the dimensions of the body the size of these non-homogeneities should be very small, which means that a clear scale separation is possible. For the moment we consider just two levels, the micro (or local) and the macro (or global) level. These levels are clearly shown in Fig. 2, where the structure is periodic and asymptotic analysis can be successfully applied. A heterogeneous medium Ω is said to have a regular periodicity if a function f

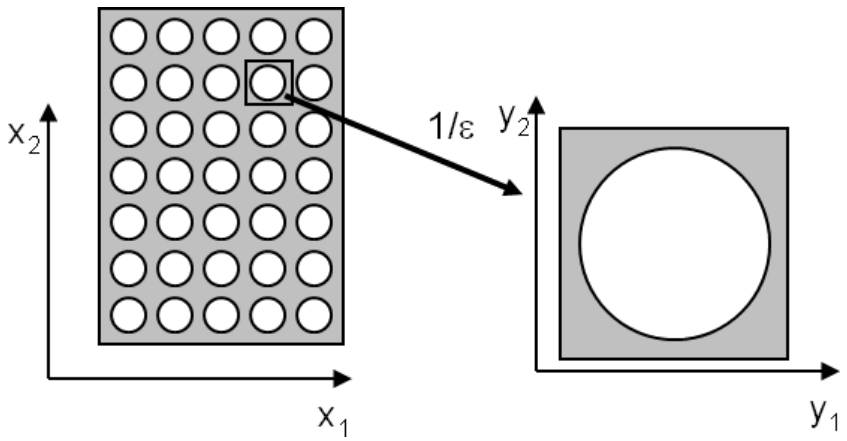

Fig. 2. Example of a periodic structure with two levels: global on the left and local on the right.

denoting some physical quantity of the medium (either geometrical or some other characteristics) has the following property:

$$\text{if } \mathbf{x} \in \Omega \quad \text{and} \quad (\mathbf{x} + \mathrm{Y}) \in \Omega \quad \text{then} \quad f(\mathbf{x} + \mathrm{Y}) = f(\mathbf{x}), \tag{19}$$

where Y is the (geometric) period of the structure. Hence, the function f is a Y-periodic function of the position vector $\mathbf{x}$ (the function f can be a scalar or vectorial or tensorial function). For example, in a composite tissued by a periodically repeating cell Y, the mechanical behaviour is described by the constitutional relations of the form:

$$\boldsymbol{\sigma}_{ij} = a_{ijkl} e_{kl} \tag{20}$$

and the tensor a_{ijkl} is a periodic function of the spatial coordinate $\mathbf{x}$, so that:

$$a_{ijkl}(\mathbf{x} + \mathrm{Y}) = a_{ijkl}(\mathbf{x}). \tag{21}$$

3.2. Statement of the problem and assumptions

One important assumption for asymptotic analysis is that it must be possible to distinguish two length scales associated with the macroscopic and microscopic phenomena. The ratio of these scales defines the small parameter (Fig. 2). Two sets of coordinates related by (22) formally express this separation of scales between macro and micro phenomena. The global coordinate vector $\mathbf{x}$ refers to the whole body and the stretched local coordinate vector $\mathbf{y}$ is related to the single, repetitive cell of periodicity:

$$\mathbf{y} = \frac{\mathbf{x}}{\varepsilon}. \tag{22}$$

In the asymptotic analysis the normalised cell of periodicity is mapped onto a sequence of finer and finer structures as ε tends to 0. If the equivalent material properties as defined below are employed, the considered fields (e.g., temperature, displacement) converge towards the homogeneous macroscopic solution as the micro-structural parameter ε tends to 0. In this sense, problems for a heterogeneous body and a homogenised one are equivalent. For more details concerning the mathematical meaning see [3] and [70].

We consider now a problem of thermo-elasticity in a heterogeneous body Ω such as that depicted in Fig. 2 defined by the equations detailed below.

– *Balance equations:*

$$\sigma^{\varepsilon}_{ij,j}(\mathbf{x}) + f_i(\mathbf{x}) = 0, \tag{23}$$

$$q^{\varepsilon}_{i,i} - r = 0. \tag{24}$$

– *Constitutive equations:*

$$\sigma^{\varepsilon}_{ij}(\mathbf{x}) = a^{\varepsilon}_{ijkl}(\mathbf{x}) e_{kl}(\mathbf{u}^{\varepsilon}(\mathbf{x})) - \alpha^{\varepsilon}_{ij}\theta, \tag{25}$$

$$q^{\varepsilon}_{i} = K^{\varepsilon}_{ij}\theta_{,j}. \tag{26}$$

– *Strain definition:*

$$e_{ij}(\mathbf{u}^{\varepsilon}(\mathbf{x})) = \frac{1}{2}\left(u^{\varepsilon}_{i,j}(\mathbf{x}) + u^{\varepsilon}_{j,i}(\mathbf{x})\right). \tag{27}$$

– *Boundary and discontinuity conditions:*

$$\begin{aligned} &\boldsymbol{\sigma}_{ij}^{\varepsilon}(\mathbf{x})n_j = 0 \quad \text{on} \quad \partial\Omega_1 \qquad \text{and} \qquad u_i^{\varepsilon}(\mathbf{x}) = 0 \quad \text{on} \quad \partial\Omega_2, \\ &q_i^{\varepsilon}(\mathbf{x})n_i = 0 \quad \text{on} \quad \partial\Omega_q \qquad \text{and} \qquad \theta^{\varepsilon}(\mathbf{x}) = 0 \quad \text{on} \quad \partial\Omega_\theta, \end{aligned} \tag{28}$$

$$\begin{aligned} &[u_i^{\varepsilon}(\mathbf{x})] = 0, \quad \left[\boldsymbol{\sigma}_{ij}^{\varepsilon}(\mathbf{x})n_j\right] = 0 \quad \text{on} \quad S_J, \\ &[\theta^{\varepsilon}(\mathbf{x})] = 0, \qquad [q_i^{\varepsilon}(\mathbf{x})n_i] = 0 \quad \text{on} \quad S_J, \end{aligned} \tag{29}$$

where Ω_1 and Ω_2 are the portions of the boundary where tractions and displacements are given respectively, on Ω_q and Ω_θ heat fluxes and temperature are given, while S_J stands for the surfaces of discontinuities of the constitutive tensors. The superscript ε is used to indicate that the variables of the problem depend on the cell dimensions related to the global length. Square parentheses denote the jump of the enclosed value. The other symbols have the usual meaning: $\mathbf{u}$ is the displacement vector, $\mathbf{e}(\mathbf{u}(\mathbf{x}))$ denotes the linearised strain tensor, $\boldsymbol{\sigma}_{ij}(\mathbf{x})$ the stress tensor, $a_{ijkl}(\mathbf{x})$ the tensor of elasticity, $K_{ij}(\mathbf{x})$ the tensor of thermal conductivity, $\alpha_{ij}(\mathbf{x})$ the tensor of thermal expansion coefficients, $\theta(\mathbf{x})$, $q_i(\mathbf{x})$ temperature and heat flux respectively, and $r(\mathbf{x})$, $f_i(\mathbf{x})$ stand for thermal sources and mass forces.

Since the components of the elasticity and thermal conductivity tensors are discontinuous, differentiation (in the above equations and in the following) should be understood in the weak sense. This is the main reason why most of the problems posed in the sequel will be presented in a variational formulation.

We introduce now the second hypothesis of homogenisation theory: we assume that the periodicity of the material characteristics imposes an analogous periodical perturbation on quantities describing the mechanical behaviour of the body; hence, we can use the following representation for displacements and temperatures:

$$\mathbf{u}^{\varepsilon}(\mathbf{x}) \equiv \mathbf{u}^0(\mathbf{x}) + \varepsilon\mathbf{u}^1(\mathbf{x},\mathbf{y}) + \varepsilon^2\mathbf{u}^2(\mathbf{x},\mathbf{y}) + ... + \varepsilon^k\mathbf{u}^k(\mathbf{x},\mathbf{y}), \tag{30}$$

$$\theta^{\varepsilon}(\mathbf{x}) \equiv \theta^0(\mathbf{x}) + \varepsilon\theta^1(\mathbf{x},\mathbf{y}) + \varepsilon^2\theta^2(\mathbf{x},\mathbf{y}) + ... + \varepsilon^k\theta^k(\mathbf{x},\mathbf{y}). \tag{31}$$

An analogous expansion with respect to powers of ε results for stresses, strains and heat fluxes:

$$\boldsymbol{\sigma}^{\varepsilon}(\mathbf{x}) \equiv \boldsymbol{\sigma}^0(\mathbf{x},\mathbf{y}) + \varepsilon\boldsymbol{\sigma}^1(\mathbf{x},\mathbf{y}) + \varepsilon^2\boldsymbol{\sigma}^2(\mathbf{x},\mathbf{y}) + ... + \varepsilon^k\boldsymbol{\sigma}^k(\mathbf{x},\mathbf{y}), \tag{32}$$

$$\mathbf{e}^{\varepsilon}(\mathbf{x}) \equiv \mathbf{e}^0(\mathbf{x},\mathbf{y}) + \varepsilon\mathbf{e}^1(\mathbf{x},\mathbf{y}) + \varepsilon^2\mathbf{e}^2(\mathbf{x},\mathbf{y}) + ... + \varepsilon^k\mathbf{e}^k(\mathbf{x},\mathbf{y}), \tag{33}$$

$$\mathbf{q}^{\varepsilon}(\mathbf{x}) \equiv \mathbf{q}^0(\mathbf{x},\mathbf{y}) + \varepsilon\mathbf{q}^1(\mathbf{x},\mathbf{y}) + \varepsilon^2\mathbf{q}^2(\mathbf{x},\mathbf{y}) + ... + \varepsilon^k\mathbf{q}^k(\mathbf{x},\mathbf{y}), \tag{34}$$

where $\mathbf{u}^k$, $\boldsymbol{\sigma}^k$,$\mathbf{e}^k$, $\boldsymbol{\theta}^k$ and$\mathbf{q}^k$ are Y – periodic, i.e., take the same values on the opposite sides of the cell of periodicity.

3.3. Asymptotic homogenisation method

The necessary mathematical tools are the chain rule of differentiation with respect to the micro variable and averaging over a cell of periodicity.

We introduce the assumption (30–34) into equations of the heterogeneous problem (23–29) and make use of the rule of a differential calculus (see also [70]), i.e., if $f = f(x,y)$ and y depends on x (in this case $y = x/\varepsilon$), then:

$$\frac{d}{dx_i}f = \left(\frac{\partial}{\partial x_i} + \frac{1}{\varepsilon}\frac{\partial}{\partial y_i}\right)f = f_{,i(x)} + \frac{1}{\varepsilon}f_{,i(y)}. \tag{35}$$

This equation explains also the notation used in the following for differentiation with respect to local and global independent variables.

Because of (35), equilibrium equations and heat balance equation split into terms of different orders (e.g., the following Eqs. (36) and (39) are of order $1/\varepsilon$). By equating the terms with the same power of ε, for the equilibrium equation we have:

$$\boldsymbol{\sigma}^0_{ij,j(y)}(\mathbf{x},\mathbf{y}) = 0, \tag{36}$$

$$\boldsymbol{\sigma}^0_{ij,j(x)}(\mathbf{x},\mathbf{y}) + \boldsymbol{\sigma}^1_{ij,j(y)}(\mathbf{x},\mathbf{y}) + f_i(\mathbf{x}) = 0, \tag{37}$$

$$\boldsymbol{\sigma}^1_{ij,j(x)}(\mathbf{x},\mathbf{y}) + \boldsymbol{\sigma}^2_{ij,j(y)}(\mathbf{x},\mathbf{y}) = 0, \tag{38}$$

...

We have similar expressions for the heat balance equation:

$$q^0_{i,i(y)}(\mathbf{x},\mathbf{y}) = 0, \tag{39}$$

$$q^0_{i,i(x)}(\mathbf{x},\mathbf{y}) + q^1_{i,i(y)}(\mathbf{x},\mathbf{y}) - r(\mathbf{x}) = 0, \tag{40}$$

$$q^1_{i,i(x)}(\mathbf{x},\mathbf{y}) + q^2_{i,i(y)}(\mathbf{x},\mathbf{y}) = 0, \tag{41}$$

...

From Eqs. (27) and (35) it follows that the main term of $\mathbf{e}$ in expansions (33) depends not only on $\mathbf{u}^0$, but also on $\mathbf{u}^1$

$$e^0_{ij}(x,y) = u^0_{(i,j)(x)} + u^1_{(i,j)(y)} \equiv e_{ij(x)}(\mathbf{u}^0) + e_{ij(y)}(\mathbf{u}^1). \tag{42}$$

The constitutive relationships (25) and (26) assume now the form:

$$\sigma^0_{ij}(\mathbf{x},\mathbf{y}) = a_{ijkl}(\mathbf{y})(e_{kl(x)}(\mathbf{u}^0) + e_{kl(y)}(\mathbf{u}^1)) - \alpha_{ij}(\mathbf{y})\theta^{\mathbf{0}}, \tag{43}$$

$$\sigma^1_{ij}(\mathbf{x},\mathbf{y}) = a_{ijkl}(\mathbf{y})(e_{kl(x)}(\mathbf{u}^1) + e_{kl(y)}(\mathbf{u}^2)) - \alpha_{ij}(\mathbf{y})\theta^{\mathbf{1}}, \tag{44}$$

...

$$q^0_k(\mathbf{x},\mathbf{y}) = K_{kl}(\mathbf{y})(\theta^0_{,l(x)} + \theta^1_{,l(y)}), \tag{45}$$

$$q^1_k(\mathbf{x},\mathbf{y}) = K_{kl}(\mathbf{y})(\theta^1_{,l(x)} + \theta^2_{,l(y)}), \tag{46}$$

...

It can be seen that the terms of order n in the asymptotic expansions for stresses (43), (44) and heat flux (45), (46) depend, respectively, on the displacement and temperature terms of order n and $n+1$. In this way the influence of the local perturbation on the global quantities is accounted for. This is the reason why for instance we need $\mathbf{u}^1\ (\mathbf{x},\mathbf{y})$ to define via the constitutive relationship the main term in expansion (32) for stresses.

3.4. Global solution

Referring separately to the terms of the same powers of ε, leads to the following variational formulations for unknowns of successive order of the problem. Starting with the first order, it can be

formally shown [70] that $\mathbf{u}^1(\mathbf{x},\mathbf{y})$ and similarly $\theta^1(\mathbf{x},\mathbf{y})$ may be represented in the following form with separated variables:

$$u_i^1(\mathbf{x},\mathbf{y}) = e_{pq(x)}(\mathbf{u}^0(\mathbf{x}))\chi_i^{pq}(\mathbf{y}) + C_i(\mathbf{x}), \tag{47}$$

$$\theta^1(\mathbf{x},\mathbf{y}) = \theta^0_{,p(x)}(\mathbf{x})\vartheta^p(\mathbf{y}) + C(\mathbf{x}), \tag{48}$$

where the functions $c_i^{pq}(\mathbf{y})$ and $\vartheta^p(\mathbf{y})$, depending only on the geometry of the cell of periodicity and on the values of the jumps of material coefficients a_{ijkl} and K_{ij} across S_J, are called functions of homogenisation for displacements and temperature, respectively.

The zero order components of the equation of equilibrium (36) and of heat balance (39) in the light of (47) and (48) yield the following boundary value problems for the functions of homogenisation:

– find $\boldsymbol{\chi}_i^{pq} \in V_Y$ such that: $\forall v_i \in V_Y$

$$\int_Y a_{ijkl}(\mathbf{y})\left(\delta_{ip}\delta_{jq} + \chi^{pq}_{i,j(y)}(\mathbf{y})\right) v_{k,l(y)}(\mathbf{y})d\Omega = 0. \tag{49}$$

– find $\vartheta^p \in V_Y$ such that: $\forall \phi \in V_Y$

$$\int_Y K_{ij}(\mathbf{y})\left(\delta_{ip} + \vartheta^p_{,i(y)}(\mathbf{y})\right)\phi_{,j(y)}(\mathbf{y})d\Omega = 0. \tag{50}$$

In the above equations, V_Y is the subset of the space of kinematically admissible functions that contains the functions with equal values on the opposite sides of the cell of periodicity Y. The homogenization functions are organized in six vectors $\boldsymbol{\chi}^{pq}$ for the displacement field and in three scalars ϑ^p for the temperature field. Functions $\boldsymbol{v}(\mathbf{y})$ and $\phi(\mathbf{y})$ are usual test functions having the meaning of Y-periodic displacements and temperature fields respectively. They are used here to write explicitly the counterparts of the expressions (36) and (39), in which the prescribed differentiations are understood in a weak sense.

The solutions $\boldsymbol{\chi}^{pq}$ and ϑ^p of the local (i.e., defined for a single cell of periodicity) boundary value problems with periodic boundary condition (49) and (50) can be interpreted as obtained for the cell subject to a unitary average strain e_{pq} and, respectively, unitary average temperature gradient $\vartheta_{,p(y)}$. The true value of perturbations are obtained after by scaling χ^{pq} and ϑ^p with true global strains (gradient of global temperature), as it is prescribed by (47) and (48).

In the asymptotic expansion for displacements (30) and for temperature (31) the dependence on $\mathbf{x}$ only is marked in the first term. The independence on $\mathbf{y}$ of these functions can be proved (see for example [70]). The functions depending only on $\mathbf{x}$ define the macro-behaviour of the structure and will be called global terms. To obtain the global behaviour of stresses and heat flux the following mean values over the cell of periodicity are defined:

$$\widetilde{\boldsymbol{\sigma}}^0(\mathbf{x}) = \frac{1}{|Y|}\int_Y \boldsymbol{\sigma}^0(\mathbf{x},\mathbf{y})dY, \qquad \widetilde{\mathbf{q}}^0(\mathbf{x}) = \frac{1}{|Y|}\int_Y \mathbf{q}^0(\mathbf{x},\mathbf{y})dY. \tag{51}$$

Averaging of equations (43) and (45) results in the following, effective constitutive relationships:

$$\widetilde{\boldsymbol{\sigma}}^0_{ij}(\mathbf{x}) = a^h_{ijkl}e_{kl}(\mathbf{u}^0) - \alpha^h_{ij}\theta^0, \qquad \widetilde{q}^0_i = -k^h_{ij}\theta^0_{,j}. \tag{52}$$

In the above equations, the effective material coefficients appear. They are computed according to:

$$a^h_{ijkl} = \frac{1}{|Y|}\int\limits_Y a_{ijpq}(\mathbf{y})(\delta_{kp}\delta_{lq} + \chi^{pq}_{k,l(y)}(\mathbf{y}))dY, \tag{53}$$

$$k^h_{ij} = \frac{1}{|Y|}\int\limits_Y k_{ip}(\mathbf{y})(\delta_{jp} + \vartheta^j_{,p}(\mathbf{y}))dY, \tag{54}$$

$$\alpha^h_{ij} = \frac{1}{|Y|}\int\limits_Y \alpha_{ij}(\mathbf{y})dY. \tag{55}$$

The macro-behaviour can be defined now by averaging equilibrium and flux balance equations (37), (40) taking into account boundary conditions (28) and finally substituting in the resulting relations the averaged counterparts of stress and heat flux (51) (it is reminded that first order terms vanish in averaging of (37), (40) because of periodicity). Equations (25) and (26) are now replaced by (52), discontinuity conditions (29) have no more sense since we deal now with homogeneous thermo-elasticity.

The heterogeneous structure can now be studied as a homogeneous one with effective material coefficients given by (53–55) and global displacements, strains and average stresses and heat fluxes can be computed. Then we go back to Eq. (43) for the recovery of the approximation of the stress field at local level. This last step is the above mentioned unsmearing or localization process.

3.5. Local approximation of the stress vector

We underline that the homogenisation approach results in two different kinds of stress tensors. The first one is the average stress field defined by $(52)_1$. It represents the stress tensor for the homogenised, equivalent body. Once the effective material coefficients are known, the global stress field and the heat flux may be obtained by means of a standard finite element thermo-mechanical code.

The second stress field is associated with a family of uniform states of strains $e_{pq(x)}$ $(\mathbf{u}^0)$ over each cell of periodicity Y. This local stress is obtained by introducing Eq. (42) into (43) and results in:

$$\sigma^0_{ij}(\mathbf{x},\mathbf{y}) = a_{ijkl}(\mathbf{y})(\delta_{kp}\delta_{lq} - \chi^{pq}_{k,l(y)})e_{pq(x)}(\mathbf{u}^0) - \alpha_{ij}(\mathbf{y})\theta^{\mathbf{0}}. \tag{56}$$

Because of (36) and (49) this tensor fulfils the equations of equilibrium everywhere in Y. If needed, the stress description can be completed with a higher order term in Eq. (32). This approach is presented in [59] and [60].

In a similar way, the local approximation of heat flux is obtained:

$$q^0_j(\mathbf{y}) = k_{ij}(\mathbf{y})(\delta_{ip} + \vartheta^p_{,i(y)}(\mathbf{y}))\theta^0_{,p(x)}. \tag{57}$$

3.6. The non linear case and bridging over several scales

Asymptotic theory of homogenisation is applicable also to non-linear situations, if applied iteratively. Further, it can be obviously used to bridge several scales. Here, we deal with the case where three scales are bridged by applying in sequential manner the two-scale asymptotic analysis. In this case, the behaviour of the components is physically non-linear and temperature dependent. Again, we refer to thermo-mechanical behaviour and introduce a micro, meso and macro level as shown in Fig. 3.

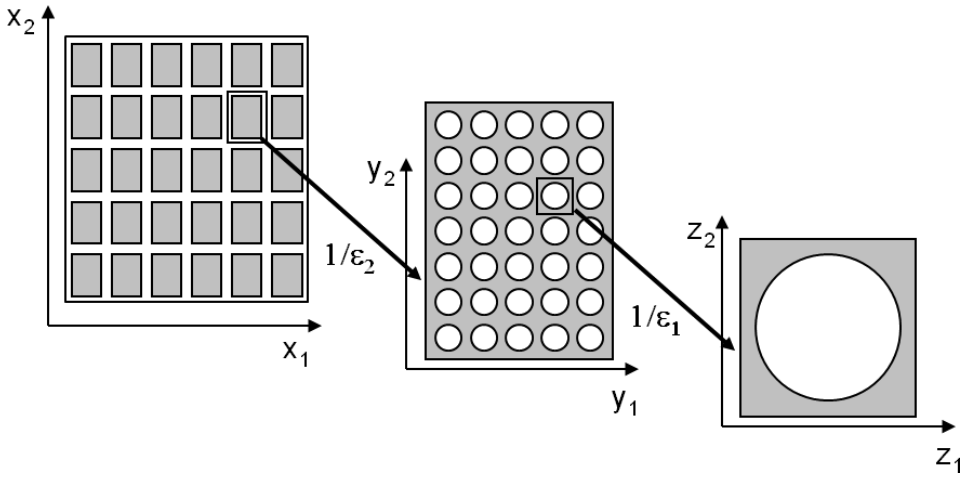

Fig. 3. Example of a periodic structure with three levels: macro (on the left), meso and micro (on the right).

At the stage of micro or meso modelling, some main features of the local structure can be extracted and used then for the macro-analysis. In order to apply the asymptotic theory, the non-linear behaviour of the components is supposed here to be piecewise linear, so that the homogenisation we perform is piecewise linear. Only monotonic loading and/or temperature change is considered, otherwise we should store the whole history and use an incremental analysis. Because of the chosen material properties, we deal with a sequence of problems of linear elasticity written for a non-homogeneous material domain and with coefficients that are functions of both temperature and strain level.

At the top level of the hierarchy, we consider an elastic body contained in the domain Ω with a smooth boundary $\partial\Omega$. The governing equations are Eqs. (23–27). For the lower level, all the formulations are formally the same with one difference: the boundary conditions are those of an infinite body. It is worth to mention that all the macro fields at the micro level become the micro fields at the higher structural level. The effective material coefficients and mean fields obtained with the homogenisation procedure at the lower level enter as local perturbations at the higher step.

Before explaining the application of the homogenisation procedure in sequential form to multi-level non-linear material behaviour we mention the solution by Terada and Kikuchi [74] who write a two-scale variational statement within the theory of homogenisation. The solution of the microscopic problem at each Gauss point of the FE mesh for the overall structure, and the deformation histories at time t_{n-1} must be stored until the macroscopic equilibrium state at current time t_n is obtained. This procedure has not been applied to bridging of more than two scales. A triple scale asymptotic analysis is used by Fish and Yu [23] to analyse damage phenomena occurring at micro-, meso- and macro scales in brittle composite materials (woven composites). These authors maintain also the second order term in the displacement expansion (Eq. (10)) and introduce a similar form for the expansion of the damage variable.

The two usual tools of homogenisation of the previous sections are used, i.e., volume averaging and total differentiation with respect to the global variable $\mathbf{x}$ that involves the local variable $\mathbf{y}$. The homogenisation functions are obtained similarly to Eqs. (49) and (50), but a factor λ is introduced in Eq. (49) to adapt the solution to the real strain level:
– find $\chi_i^{pq} \in V_Y$ such that:

$$\forall v_i \in V_Y \int\limits_{Y(\lambda)} C_{ijkl}(\mathbf{y}, \lambda, \theta^0) \left(\delta_{ip}\delta_{jq} + \chi^{pq}_{i,j(y)}\right) v_{k,l(y)} d\Omega = 0, \qquad \sigma(\lambda, \chi_i^{pq}) \in P. \tag{58}$$

Material properties depend upon temperature, so that a set of representative temperatures is considered for the material input data and linear interpolation is used between the given values.

P is the domain inside the surface of plasticity. The requirement that the stress belongs to the admissible region P (introduced in (58)) is verified via classical unsmearing procedure, described in the preceding section.

The modification of the algorithm required by the non-linearity is now explained. We start with the composite cell of periodicity with given elastic components. The uniform strain is increased step by step. Effective material coefficients are constant until the stress reaches the yield surface in some points of the cell. The yield surface in the space of stresses is different for each material component, being thus a function of place. The region, where the material yields, is of finite volume at the end of the step, so it is easy to replace the material with the yielded one, with the elastic modulus equal to the hardening one and with Poisson's ratio tending to 0.5.

The cell of periodicity is hence changed: it is made up of one more material and we can start the usual analysis again (uniform strain, new homogenisation functions, new stress map over the cell). We identify then the new region where further local yielding occurs, then redefine the cell, etc. The loop is repeated as many times as needed. In (58) the history of this replacement of materials at the micro level is marked by λ, the level of the average stress, for which the micro yielding occurs each time. At the end of each step we can compute also the mean stress over the cell having (generalised) homogenisation functions (see Eq. (52)) and the effective coefficients can be computed using Eqs. (53), (54) and (55). The algorithm is summarised in Box 1.

1. Compute effective coefficients at micro level;
2. Compute effective coefficients at meso level;
3. Apply increment of forces and/or temperature at the macro level, solve global homogeneous problem;
4. Compute global strain E_{ij}^{macro}: $E_{ij}^{macro} = e_{ij}(\mathbf{u}^0)$;
5. Apply E_{ij}^{macro} to a single meso- level cell by equivalent kinematical loading (displacement on the border);
6. Solve the kinematical problem at the meso level on the unit cell, compute stress (unsmearing for meso level) and strain E_{ij}^{macro};
7. Apply E_{ij}^{macro} to micro- level cell by equivalent kinematical loading (displacements on the border);
8. Solve the kinematical problem at the micro level for $\mathbf{u}^1(\mathbf{z})$, compute stress (unsmearing for micro level);
9. Verify yielding of the material in the physically true situation at micro level. If yes, change mechanical parameter of the material and go to 1, if else exit.

Box 1: Algorithm for the three-scale homogenization in case of non linear material behaviour.

As mentioned previously for the two-scale analysis, an important part of multi-scale modelling is the recovery of stress and heat flux as well as strain, temperature and displacements at the level of the microstructure. In the linear case, it has been shown that the homogenisation functions are obtained as a solution of a series of boundary value problems (BVPs) with periodic boundary conditions formulated over a cell of periodicity. The vector of homogenisation functions allows also to retrieve the local field of stress and strain on the cell of periodicity at each structural level and for each value of the mean strain field at hand. When the material behaviour is not elastic, the homogenisation functions cannot be applied. The local fields can be obtained numerically, e.g., by solving a BVP for the cell of periodicity loaded with a distribution of displacements corresponding to the mean strain field computed for the preceding level of the hierarchy (see Box 1). Because of the three-level hierarchical structure we are dealing with, the recovery process must be applied twice, and since material characteristics are temperature dependent and non linear, the procedure must be applied for each representative temperature and within the context of the correct stress state. Therefore, this part is computationally very expensive: it must be performed at the end of each step of the global analysis until the micro-scale, to verify if yielding is taking place or evolving at the lowest level. To speed up this procedure, artificial neural networks can be used. Interested readers can find in [58, 13, 8] the details of this approach.

Concerning the preservation of thermodynamic consistency in case of asymptotic expansion, it appears to be still an open problem. It is worth to point out that with the asymptotic method we formulate an effective constitutive relation (not only coefficients) in a fully consequential manner. Therefore for problems like, e.g., linear thermo-elasticity, the results are thermodynamically consistent, but more complicated situations should be individually analysed. In the asymptotic analysis, as ε tends to 0 the normalized cell of periodicity is mapped onto a sequence of finer and finer structures and the considered fields (temperature, displacement) converge towards the homogeneous macroscopic solution. However, the expansion is usually truncated after a few terms, pointing out that what matters here is the size of the unit cell. As long as it is infinitesimally small, it is generally accepted that the 0(1) theory is as good as anything else. The problem is the finite size of the cell which usually appears in numerical exploitation of the method. Here the question is still open as it is in the case of numerical multi-scale procedures like those mentioned at the beginning of this paper.

4. Numerical examples

4.1. Drying shrinkage of concrete

In the first example, we consider drying shrinkage of young concrete where a proper choice of the stress tensor allows avoiding the need for an experimentally obtained shrinkage coefficient (valid only for each particular material) linking relative humidity with shrinkage strain. However, the functional dependence of the Helmholtz free energy must be sufficiently rich to properly represent the physical reality. The stress form obtained by Coussy [19]:

$$d\mathbf{t}^{ef} = d\mathbf{t}^{tot} + \alpha \left(dp^g - S_w dp^c\right) \mathbf{I} \tag{59}$$

with a Helmholtz free energy for the solid phase depending only on S_w the water degree of saturation, T the absolute temperature and $\mathbf{E}_s$ the Lagrangian strain tensor, is not sufficient to simulate the strain behaviour at low values of relative humidity. On the other hand, the generalised Skempton stress tensor containing the disjoining pressure, Eq. (16), where the Helmholtz free energy depends also on the specific interface areas [40] allows following the experimentally observed strain behaviour down to very low values of the relative humidity [33], Fig. 4. Application of the effective stress theory by Gray and Schrefler [41] allows also for efficient analysis of such difficult problems like for example creep phenomena in maturing concrete due to autogeneous shrinkage [30, 33], or thermo-chemical degradation of concrete at high temperature [27, 29].

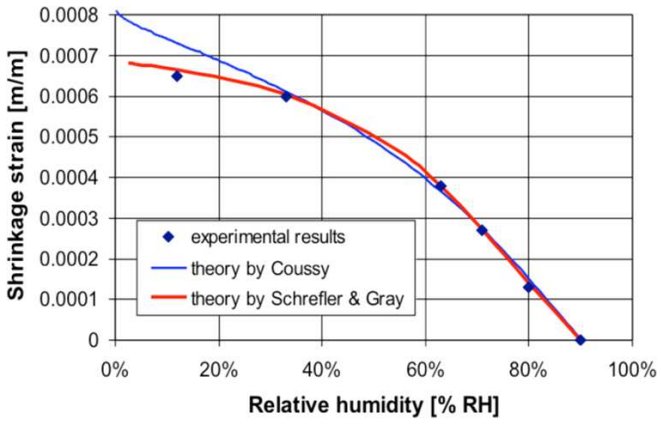

Fig. 4. Drying process of a concrete sample: comparison between experimental values and numerical results obtained according to the theories [19] and [33].

4.2. Leaching of concrete

The second example deals with calcium leaching of concrete which is particularly important for containment structures for nuclear waste disposal. Equilibrium based models show convergence problems because of the sudden appearance of large source terms which must attain equilibrium instantaneously. Models which consider thermodynamic imbalance of the calcium in solid and liquid phases, allowing for the description of process kinetics behave numerically much better [33–35]. The correct evolution of the chemical process is captured through the introduction, for each chemical component, of the relaxation time which would be zero in equilibrium type models but not in reality and in process kinetics based models. As additional bonus of this kind of approach, it allows for introducing non isothermal leaching by means of the thermal diffusion of ionic species and the temperature dependence of the chemical reaction through an Arrhenius-like relationship.

As an example we show the case of non-isothermal leaching of a cubic specimen (side = 4 cm) in direct contact with deionised water at two different temperatures: 25°C and 60°C. For further information about material properties and boundary conditions used in the numerical simulation, see [34]. Figures 5 and 6 show the calcium content in the solid skeleton and in the saline solution after 7500 days. As can be observed, calcium leaching process is strongly dependent on the temperature, and the mathematical model, based on the Volume Averaging theory, allows efficient numerical analysis of the chemical degradation induced by the process.

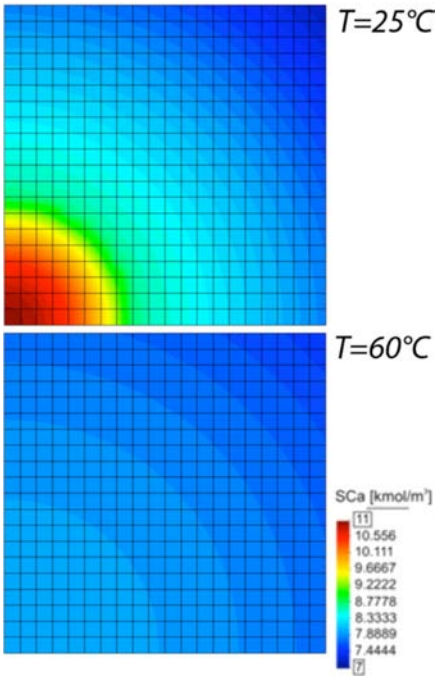

Fig. 5. Calcium concentration in the liquid solution after 7500 days at two different temperatures [34].

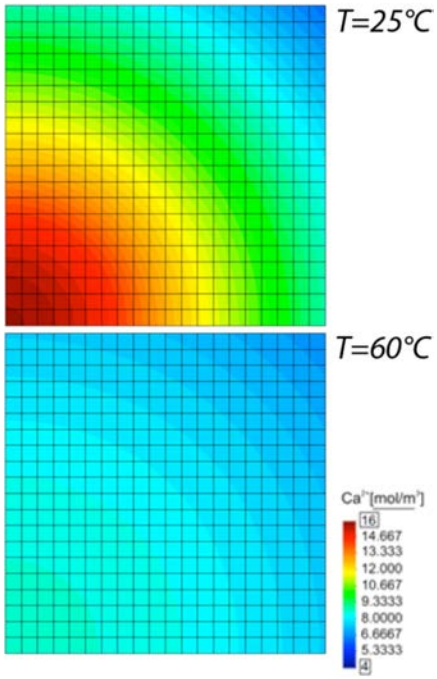

Fig. 6. Calcium concentration in the liquid solution after 7500 days at two different temperatures [34].

4.3. Three-scale asymptotic homogenization

The third case deals with the thermo-mechanical analysis of a superconducting strand used in the coils of the International Thermo-nuclear Experimental Reactor (ITER), which is now under construction. ITER is a tokamak type reactor, which uses magnetic confinement of the plasma. To this purpose, strong magnetic fields are produced by coils formed by winding superconducting cables. Cables are formed by more than one thousand strands twisted together according to a multi-level scheme. Strands are usually made of a resistive matrix (bronze in most cases) where superconducting filaments are embedded. In most of ITER magnets Nb3Sn based strands will be

used and it is well known that the critical parameters of Nb_3Sn are strain sensitive; experimental investigations on short samples of basic strands and sub-size cables already demonstrated the significant effects of residual strain on the critical parameters [72]. This Nb_3Sn sensitivity to strain leads to considerable problems in accurate performance prediction when the strands are used in large multi-strand CIC conductors at high field. Besides damage phenomena in the filament [17, 64] and complex stress-strain fields within the cable (and therefore in the Nb_3Sn filaments) created by the pulsing magnetic forces [2, 63], there are also interaction phenomena due to the different thermal contraction coefficients of the various materials. Thermal strain state due to the heat treatment of the strands plays a fundamental role on the final characteristics of the cable and its performances in working conditions; therefore, a good estimation of these strains is compulsory.

In the strand (Fig. 7) a three-level hierarchy can be identified [5–8, 14]: the single filament (micro-scale, on the right), groups of filaments (meso-scale, in the centre) and the superconducting strand (macro-scale, on the left). In this example, we compute the effective characteristics and the strain field due to the cool down of a single strand from its reaction temperature (Nb_3Sn is formed at 923 K) to the coil working condition (4.2 K). The additional strain field due to Lorentz force, originating when the coil is energized, is analysed in [68, 78]. The problem of interaction among many strands is left apart and can be dealt with as studied in [15, 16, 79]. We assume that the strand components are in equilibrium at 923 K without eigenstresses or eigenstrains, which are relaxed since the strand remains for several hours at high temperature. We have to deal with non-linear, temperature-dependent material characteristics.

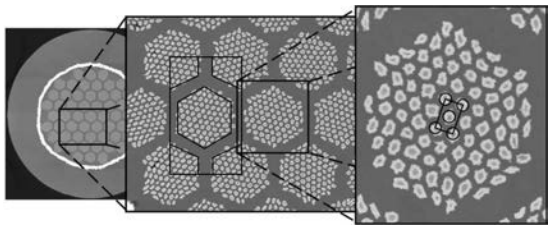

Fig. 7. Three level hierarchy in the superconducting strand. The central part of the strand itself (left) consists of 55 groups of 85 filaments (about 4 micrometers diameter), embedded in a bronze matrix, while the outer region is made of high conductivity copper and is separated by the inner one by a tantalum barrier. Images: courtesy of P.J. Lee, University of Wisconsin–Madison Applied Superconductivity Center.

Asymptotic theory of homogenisation is adopted for the non linear situation and the three scales are bridged by applying it in concurrent manner. The repeating unit cell (RUC) for the micro- and meso-level are shown in Fig. 8. The obtained effective characteristics are presented in Fig. 9. Finally

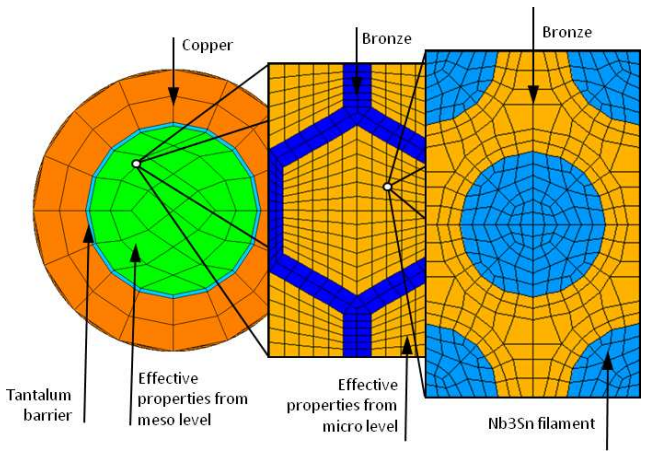

Fig. 8. Finite element mesh of micro- (on the right) and meso- (in the middle) scale unit cell. The discretization used for the macro level computations is shown on the left.

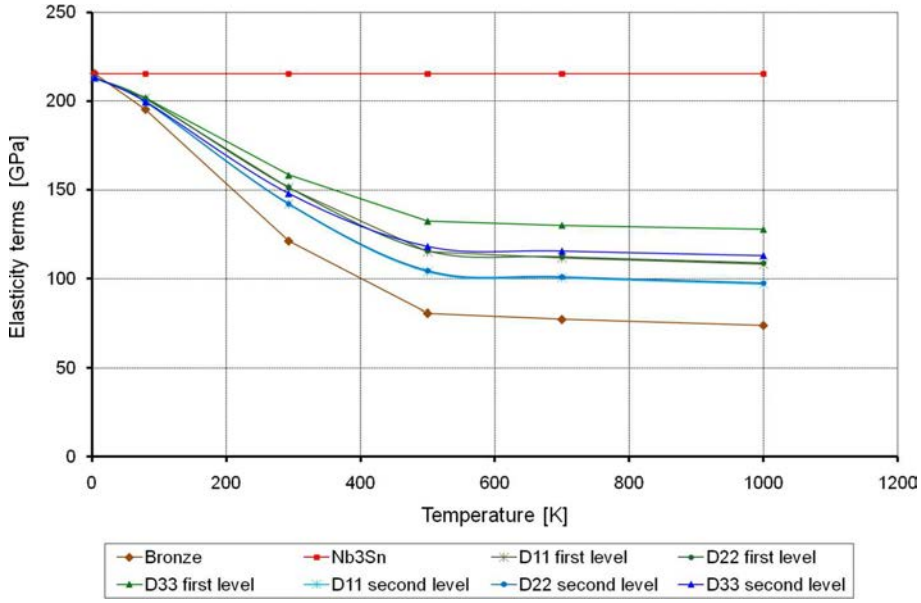

Fig. 9. Homogenization results for diagonal terms of elasticity matrix: first level (green lines) and second level (blue lines). Initial materials (bronze and Nb_3Sn) are also shown.

the computed and measured residual strains, after the cool down process, are compared in Fig. 10; it shows that the results are remarkably accurate.

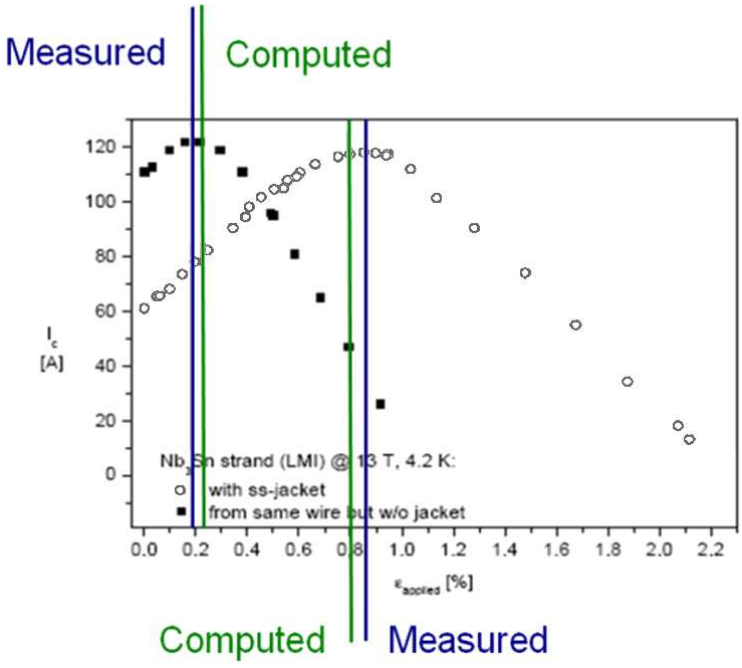

Fig. 10. Computed and measured residual strain.

5. Concluding remarks

It is not straightforward to maintain thermodynamic consistency in multiphysics and multi-scale mathematical models. Theoretical fundamentals of two different approaches assuring thermodynamic consistency are briefly summarised: Hybrid Mixture Theory based on space averaging, which

can be applied for modeling chemo-hygro-thermo-mechanical problems of multiphase porous materials, and Asymptotic Theory of Homogenisation, allowing analysis of hierarchical thermo-mechanical problems.

Its importance is now generally admitted in computational mechanics and is exploited in CFD since a long time ago. In fluid structure interaction problems with interaction in the domain, it is pursued mainly when writing the mathematical multi-scale model. This quest for thermodynamic consistency has led to improved models for simulating drying shrinkage through adoption of a more appropriate stress tensor which includes disjoining pressure. Adoption of thermodynamic non-equilibrium approach has then permitted to simulate non-isothermal leaching in concrete and has led to models which show less convergence difficulties.

Finally, the preservation of thermodynamic consistency in case of asymptotic expansion, appears to be still an open problem, worth to be investigated. In the asymptotic analysis, the expansion is usually truncated after a few terms, pointing out that what matters here is the size of the unit cell. As long as it is infinitesimally small, it is generally accepted that the 0(1) theory is as good as anything else. The problem is the finite size of the cell which usually appears in numerical exploitation of the method. Here, the question is still open as it is in the case of other numerical multi-scale procedures like those mentioned at the beginning of this paper.

Acknowledgements

Support for this work was partially provided by Italian Research Grant STPD08JA32_004 "Algorithms and Architectures for Computational Science and Engineering". This support is gratefully acknowledged. The authors wish to thank Prof. Ramon Codina for the information regarding thermodynamics and CFD.

References

[1] P. Baggio, C. Bonacina, B.A. Schrefler. Some considerations on modeling heat and mass transfer in porous media. *Transport in Porous Media*, **28**: 233–251, 1997.

[2] F. Bellina, D. Boso, B.A. Schrefler, G. Zavarise. Modeling a multistrand SC cable with an electrical DC lumped network. *IEEE Trans. Appl. Supercond.*, **12**(1): 1408–12, 2002.

[3] A. Bensoussan, J.L. Lions, G. Papanicolau. *Asymptotic Analysis for Periodic Structures*. North-Holland, Amsterdam, 1976.

[4] R.I. Borja. Cam-clay plasticity. Part V: a mathematical framework for three-phase deformation and strain localization analyses of partially saturated porous media. *Comput. Methods Appl. Mech. Engrg*, **193**: 5301–5338, 2004.

[5] D.P. Boso, M. Lefik, B.A. Schrefler. A multilevel homogenised model for superconducting strand thermomechanics, *Cryogenics*, **45**(4): 259–271, 2005.

[6] D.P. Boso, M. Lefik, B.A. Schrefler. Multiscale analysis of the influence of the triplet helicoidal geometry on the strain state of a Nb_3Sn based strand for ITER coils. *Cryogenics*, **45**(9): 589–605, 2005.

[7] D.P. Boso, M. Lefik, B.A. Schrefler. Homogenisation methods for the thermo-mechanical analysis of Nb_3Sn strand. *Cryogenics*, **46**(7–8): 569–80, 2006.

[8] D.P. Boso, M. Lefik, B.A. Schrefler. Thermo-mechanics of the hierarchical structure of ITER superconducting cables. *IEEE Trans. Appl. Supercond.*, **17**(2): 1362–5, 2007.

[9] D.P. Boso, M. Lefik, B.A. Schrefler. Generalized self-consistent like method for mechanical degradation of fibrous composites. *ZAMM Zeitschrift fur Angewandte Mathematik und Mechanik*, **91**(12): 967–78, 2011.

[10] D.P. Boso, M. Lefik, B.A. Schrefler. Recent developments in numerical homogenization. *Comput. Assis. Mech. Eng. Sci.*, **16**(3–4): 161–83, 2009.

[11] D.P. Boso, M. Lefik, B.A. Schrefler. Generalised self consistent homogenisation as an inverse problem. *ZAMM Zeitschrift fur Angewandte Mathematik und Mechanik*, **90**(10–11): 847–60, 2010.

[12] D.P. Boso, M. Lefik. A thermo-mechanical model for Nb3Sn filaments and wires: Strain field for different strand layouts. *Superconductor Science and Technology*, **22**(12), article number 125012, 2009.

[13] D.P. Boso, M. Lefik. Numerical phenomenology: Virtual testing of the hierarchical structure of a bundle of strands. *CMES – Computer Modeling in Engineering and Sciences*, **55**(3): 319–37, 2010.

[14] D.P. Boso, M. Lefik, B.A. Schrefler. Thermal and bending strain on Nb_3Sn strands. *IEEE Trans. Appl. Supercond.*, **16**(2): 1823–7, 2006.

[15] D.P. Boso, G. Zavarise, B.A. Schrefler. A formulation for electrostatic-mechanical contact and its numerical solution. *Int. J. Numer. Methods Eng.*, **64**(3): 382–400, 2005.

[16] D.P. Boso, P. Litewka, B.A. Schrefler, P. Wriggers. A 3D beam-to-beam contact finite element for coupled electric-mechanical fields. *Int. J. Numer. Methods Eng.*, **64**(13): 1800–15, 2005.

[17] D. Boso, C. Pellegrino, U. Galvanetto, B.A. Schrefler. Macroscopic damage in periodic composite materials. *Communications in Numerical Methods in Engineering*, **16**(9): 615–23, 2000.

[18] W. Chen, J. Fish. A dispersive model for wave propagation in periodic heterogeneous media based on homogenization with multiple spatial and temporal scales. *Journal of Applied Mechanics*, **68**: 153–161, 2001.

[19] O. Coussy. *Mechanics of Porous Continua*. Wiley, Chichester, 1995.

[20] O. Coussy. *PoroMechanics*, Wiley, Chichester, 2004.

[21] R. de Boer, W. Ehlers, S. Kowalski, J. Plischka. Porous media, a survey of different approaches. *Forschungsbericht aus dem Fachbereich Bauwesen*, **54**, Universität-Gesamthochschule Essen, 1991.

[22] J.D. Eshelby. The determination of the elastic field of an ellipsoidal inclusion and related problems. *Proc. Roy. Soc.*, **A241**: 376–396, 1957.

[23] J. Fish, Q. Yu. Multiscale Damage Modeling for Composite Materials: Theory and Computational Framework. *Int. J. Num. Meth. Engn.*, **52**(1–2): 161–192, 2001.

[24] D. Gawin, P. Baggio, B.A. Schrefler. Coupled heat, water and gas flow in deformable porous media. *Int. J. Num. Meth. in Fluids*, **20**: 969–987, 1995.

[25] D. Gawin, M. Lefik, B.A. Schrefler. ANN approach to sorption hysteresis within a coupled hygro-thermo-mechanical FE analysis. *Int. J. Num. Meth. Engrg*, **50**: 299–323, 2001.

[26] D. Gawin, C.E. Majorana, B.A. Schrefler. Numerical Analysis of Hygro-Thermic Behaviour and Damage of Concrete at High Temperature. *Mech. Cohes.-Frict. Mater.*, **4**: 37–74, 1999.

[27] D. Gawin, F. Pesavento, B.A. Schrefler. Modelling of Hygro-Thermal Behaviour and Damage of Concrete at Temperature Above the Critical Point of Water. *Int. J. Numer. Anal. Meth. Geomech.* **26**: 537–562, 2002.

[28] D. Gawin, F. Pesavento, B.A. Schrefler. Modelling of hygro-thermal behaviour of concrete at high temperature with thermo-chemical and mechanical material degradation. *Comput. Methods Appl. Mech. Engrg.*, **192**: 1731–1771, 2003.

[29] D. Gawin, F. Pesavento, B.A. Schrefler. Modelling of deformations of high strength concrete at elevated temperatures. *Mat. Struct.*, **37**(268): 218–236, 2004.

[30] D. Gawin, F. Pesavento, B.A. Schrefler. Hygro-thermo-chemo-mechanical modelling of concrete at early ages and beyond. Part I: Hydration and hygro-thermal phenomena. *Int. J. Num. Meth. Engrg.*, **67**(3): 299–331, 2006.

[31] D. Gawin, F. Pesavento, B.A. Schrefler. Hygro-thermo-chemo-mechanical modelling of concrete at early ages and beyond. Part II: Shrinkage and creep of concrete. *Int. J. Num. Meth. Engrg.*, **67**(3): 332–363, 2006.

[32] D. Gawin, F. Pesavento, B.A. Schrefler. Towards prediction of the thermal spalling risk through a multi-phase porous media model of concrete. *Comput. Methods Appl. Mech. Engrg.*, **195**(41–43): 5707–5729, 2006.

[33] D. Gawin, F. Pesavento, B.A. Schrefler. Modelling creep and shrinkage of concrete by means of effective stresses. *Mater. Struct.*, **40**(6): 579–591, 2007.

[34] D. Gawin, F. Pesavento, B.A. Schrefler. Modeling of cementitious materials exposed to isothermal calcium leaching, with considering process kinetics and advective water flow. Part 1: Theoretical model. *Int. J. Solids Struct.*, **45**(25–26): 6221–6240, 2008.

[35] D. Gawin, F. Pesavento, B.A. Schrefler. Modeling of cementitious materials exposed to isothermal calcium leaching, with considering process kinetics and advective water flow. Part 2: Numerical solution. *Int. J. Solids Struct.*, **45**(25–26): 6241–6268, 2008.

[36] D. Gawin, F. Pesavento, B.A. Schrefler. Modeling deterioration of cementitious materials exposed to calcium leaching in non-isothermal conditions. *Comput. Methods Appl. Mech. Engrg.*, **198**: 3051–3083, 2009.

[37] D. Gawin, L. Sanavia. A unified approach to numerical modeling of fully and partially saturated porous materials by considering air dissolved in water. *CMES – Computer Modeling in Engineering & Sciences*, **53**(3): 255–302, 2009.

[38] W.G. Gray, S.M. Hassanizadeh. Unsaturated flow theory including interfacial phenomena, *Water Resour. Res.*, **27**: 1855–1863, 1991.

[39] W.G. Gray, C.T. Miller. Thermodynamically constrained averaging theory approach for modeling flow and transport phenomena in porous medium systems: 1. Motivation and overview. *Advances in Water Resources*, **28**: 161–180, 2005.

[40] W.G. Gray, B.A. Schrefler, F. Pesavento. The solid stress tensor in porous media mechanics and the Hill-Mandel condition. *J. of the Mechanics and Physics of Solids*, **57**: 539–544, 2009.

[41] W.G. Gray, B.A. Schrefler. Analysis of the solid phase stress tensor in multiphase porous media. *Int. J. Numer. Anal. Meth. Geomech.*, **31**(4): 541–581, 2007.

[42] J.L. Guermond, webpage: http://www.math.tamu.edu/∼guermond.

[43] Z. Hashin, S. Shtrikman, A. Variational. Approach to the theory of the Elastic Behaviour of Multiphase Materials. *J. Mech. Phys. Sol.*, **11**(2): 127–141, 1964.

[44] S.M. Hassanizadeh, W.G. Gray. Mechanics and thermodynamics of multiphase flow in porous media including interphase boundaries. *Advances in Water Resources*, **13**(4): 169–186, 1990.

[45] S.M. Hassanizadeh, W.G. Gray. General Conservation Equations for Multi-Phase Systems: 1. Averaging Procedure. *Advances in Water Resources*, **2**: 131–144, 1979.

[46] S.M. Hassanizadeh, W.G. Gray. General Conservation Equations for Multi-Phase Systems: 2. Mass, Momenta, Energy and Entropy Equations. *Advances in Water Resources*, **2**: 191–203, 1979.

[47] S.M. Hassanizadeh, W.G. Gray. General Conservation Equations for Multi-Phase Systems: 3. Constitutive Theory for Porous Media Flow. *Advances in Water Resources*, **3**: 25–40, 1980.

[48] T.J.R. Hughes, M. Mallet, L.P. Franca. Entropy-stable finite element methods for compressible fluids: application to high order Mach number flows with shocks, In: P.G. Bergan, K.J. Bathe, W. Wunderlich, eds., *Finite Element Methods for Nonlinear Problems*, 761–773. Springer, Berlin, 1986.

[49] T.J.R. Hughes, L.P. Franca, M. Mallet. A new finite element formulation for computational fluid dynamics: I. Symmetric forms of the compressible Euler and Navier–Stokes equations and the second law of thermodynamics. *Comput. Methods Appl. Mech. Engrg.*, **54**: 223–234, 1986.

[50] K. Hutter, L. Laloui, L. Vulliet. Thermodynamically based mixture models of saturated and unsaturated soils. *Mech. Cohesive-Frict. Mater.*, **4**: 295–338, 1999.

[51] C. Johnson, A. Szepessy. On the convergence of a finite element Method for a nonlinear hyperbolic conservation law. *Math. Comp.*, **49**: 427–444, 1987.

[52] P. Kanouté, D.P. Boso, J.L. Chaboche, B.A. Schrefler. Multiscale Methods for Composites: a Review. *Archives of Computational Methods in Engineering.* **16**(1): 31–75, 2009.

[53] M. Koniorczyk, D. Gawin. Heat and moisture transport in porous building materials containing salt. *Journal of Building Physics*, **31**(4): 279–300, 2008.

[54] M. Koniorczyk, D. Gawin. Numerical modeling of salt transport and precipitation in non-isothermal partially saturated porous media considering kinetics of salt phase changes. *Transport in Porous Media*, **87**(1): 57–76, 2011.

[55] E. Kröner. Bounds for Effective Elastic Moduli of Disordered Materials. *J. Mech. Phys. Sol.*, **25**(2): 137–155, 1977.

[56] E. Kröner. Self-consistent scheme and graded disorder in polycristal elasticity. *J. Phys. F.*, **8**: 2261–2267, 1978.

[57] M. Lefik, D.P. Boso, B.A. Schrefler. Generalized self-consistent homogenization using the finite element method. *ZAMM Zeitschrift fur Angewandte Mathematik und Mechanik*, **89**(4): 306–19, 2009.

[58] M. Lefik, D.P. Boso, B.A. Schrefler. Artificial neural networks in numerical modelling of composites. *Comput. Methods Appl. Mech. Engng.*, **198**(21–26): 1785–1804, 2009.

[59] M. Lefik, B.A. Schrefler. 3D Finite Element Analysis of Composite Beams with Parallel Fibres Based on the Homogenisation Theory. *Computational Mechanics*, **14**(1): 2–15, 1994.

[60] M. Lefik, B.A. Schrefler. Application of the Homogenisation Method to the Analysis of Superconducting Coils. *Fusion Engineering and Design*, **24**: 231–255, 1994.

[61] W.K. Liu, D. Qian, S. Gonella, S.F. Li, W. Chen, S. Chirputkar, Multiscale methods for mechanical science of complex materials: Bridging from quantum to stochastic multiresolution continuum. *Int.J. Numer. Meth. Engng.*, **83**(8–9): 1039-1080, 2010.

[62] T. Mori, K. Tanaka. Average Stress in Matrix and Average Elastic Energy of Materials with Misfitting Inclusions. *Acta Metallurgica*, **21**: 571–574, 1973.

[63] A.S. Nemov, D.P. Boso, I.B. Voynov, A.I. Borovkov, B.A. Schrefler. Generalized stiffness coefficients for ITER superconducting cables, direct FE modeling and initial configuration. *Cryogenics*, **50**(5): 304–13, 2010.

[64] C. Pellegrino, U. Galvanetto, B.A. Schrefler, Numerical homogenisation of periodic composite materials with non-linear material components. *Int. J. Num. Meth. Engng.*, **46**, 1609–1637, 1999.

[65] F. Pesavento, D. Gawin, B.A. Schrefler. Modeling cementitious materials as multiphase porous media: theoretical framework and applications. *Acta Mechanica*, **201**(1–4): 313–339, 2008.

[66] R.C. Picu. Foreword to Special Issue on Linking Discrete and Continuum Models. *Int. J. Multiscale Computational Engng.*, **1**(1): VII–VIII, 2003.

[67] A. Reuss. Berechnung der Fliessgrenze von Mischkristallen auf grund der Plastizitatsdingung fur Einkristalle. *Z. Angew. Math. Mech.*, **9**: 49, 1926.

[68] P.L. Ribani, D.P. Boso, M. Lefik, Y. Nunoya, L. Savoldi Richard, B.A. Schrefler, R. Zanino . THELMA code analysis of bronze route Nb_3Sn strand bending effect on I_c. *IEEE Trans. Appl. Supercond.*, **16**(2): 860–863, 2006.

[69] L. Sanavia, F. Pesavento, B.A. Schrefler. Finite element analysis of non-isothermal multiphase geomaterials with application to strain localization simulation. *Computational Mechanics*, **37**(4): 331–348, 2005.

[70] E. Sanchez-Palencia. *Non-Homogeneous Media and Vibration Theory.* Springer, Berlin, 1980

[71] B.A. Schrefler. Mechanics and thermodynamics of saturated-unsaturated porous materials and quantitative solutions. *Appl. Mech. Rev.*, **55**(4): 351–388, 2002.

[72] W. Specking, J.L Duchateau and P. Decool. Critical current vs. strain tests on EU strands and subsize Cable-in-Condiuts with stainless steel and incoloy jackets. *GB5-M27 ITER taskN. NIITT45, Final report*, October 1997.

[73] A. Szepessy. *Convergence of the streamline diffusion finite element method for conservation laws*, PhD. Thesis, Mathematics Department, Chalmers University of Technology, Göteborg, 1989.

[74] K. Terada, N. Kikuchi. A class of general algorithms for multi-scale analyses of heterogeneous media. *Comput. Methods Appl. Mech. Engrg.*, **190**: 5427–5464, 2001.

[75] W. Voigt. *Lehrbuch der Kristallphysik*. Teubner-Leipzig-Berlin, 1910.

[76] J.R. Willis. Bounds and self-consistent estimates for the overall properties of anisotropic composites. *J. Mech. Phys. Sol.*, **25**: 185–202, 1977.

[77] M. Xu, R. Gracie, T. Belytschko. A continuum-to-atomistic bridging domain method for composite lattices. *Int. J. Numer. Meth. Engrg.*, **81**(13): 1635–1658, 2010.

[78] R. Zanino, D.P. Boso, M. Lefik, P.L. Ribani, L. Savoldi Richard, B.A. Schrefler. Analysis of bending effects on performance degradation of ITER-relevant Nb_3Sn strand using the THELMA code. *IEEE Trans. Appl. Supercond.*, **18**(2): 1067–1071, 2008.

[79] H.W. Zhang, D.P. Boso, B.A. Schrefler. Homogeneous Analysis of Periodic Assemblies of Elastoplastic Disks in Contact. *International Journal for Multiscale Computational Engineering*, **1**(4): 349–370, 2003.

[80] H.W. Zhang, S. Zhang, J.Y. Bi, B.A. Schrefler. Thermo-mechanical analysis of periodic multiphase materials by a multiscale asymptotic homogenization approach. *Int. J. Numer. Meth. Engrg.*, **69**(1): 87–113, 2007.